



Research paper

A “turn-on” fluorescence sensor for Pb²⁺ detection based on graphene quantum dots and gold nanoparticles



Xiaofang Niu, Yuanbo Zhong, Rui Chen, Fei Wang, Yanjun Liu, Dan Luo*

Department of Electrical and Electronic Engineering, Southern University of Science and Technology, Xueyuan Road 1088, Nanshan District, Shenzhen, Guangdong, 518055, PR China

ARTICLE INFO

Article history:

Received 5 March 2017

Received in revised form 4 August 2017

Accepted 22 August 2017

Available online 26 August 2017

Keywords:

Lead

Fluorescence sensor

Graphene quantum dots

Gold nanoparticles

ABSTRACT

Heavy metal, such as Pb²⁺, detection technologies are quite important in environment monitoring and human health protection. However, most existing technologies are often time consuming, expensive with sophisticated equipment, and requirement of complicated sample pre-treatment, which limit the useful range of real-time application. Here, we report the development of a “turn-on” fluorescence sensor for Pb²⁺ detection based on graphene quantum dots and gold nanoparticles. We achieved an extremely broad detection range of Pb²⁺ from 50 nM to 4 μM, with a detection limit of 16.7 nM. This sensing system is highly sensitive and selective for determination of Pb²⁺. The proposed strategy is expected to provide considerable implication for other heavy metal, antigen, or DNAs by modifying sensing molecules, and fast examination in chemical and biological applications.

© 2017 Elsevier B.V. All rights reserved.

1. Introduction

Lead is one of the major environmental pollutants origins from gasoline, batteries and industrial pigments, accompanying by severe human health risks including muscle paralysis, memory loss, anemia, cardiovascular dysfunction and mental troubles [1–3]. Therefore, quantitative and sensitive detection is important, particularly in aqueous environments. Many technologies have been developed for the detection of lead ions (Pb²⁺), such as atomic absorption spectroscopy (AAS) [4], plasma atomic emission spectroscopy [5], surface enhanced Raman spectroscopy [6], anodic stripping voltammetry [7], colorimetric [8], biochemical [9], and electrochemical techniques [10], but these methods are time consuming, expensive with sophisticated equipment, and may require complicated sample pre-treatment. Therefore, developing novel method for Pb²⁺ real-time sampling is highly desirable. Recently, fluorescence spectrometry has attracted considerable interests due to its simplicity, low-cost and high sensitivity and selectivity [11]. The naked-eye fluorescence sensor for Pb²⁺ detection is a promising method in fields of clinical toxicology, environmental monitoring and industry process monitoring.

Grapheme quantum dots (GQDs) [12–15] have attracted considerable interest for developing various applications in biological

imaging [16], sensor [17], phototransistors [18] and photovoltaic devices [19] in recent years. Comparing to conventional fluorescence probes such as organic dyes and inorganic semiconductor quantum dots, which are hindered from drawbacks as such poor photostability, easy photobleaching, and short lifetime, GQDs exhibit great advantage due to their intrinsic superiorities such as high photoluminescence, excellent biocompatibility, good resistance to photobleaching, and stable emission [20–23]. Therefore, GQDs are expected to be excellent alternatives to organic dyes and semiconductor QDs for fluorescence sensor both in biological system and heavy metal detection.

Herein, for the first time, we develop a “turn on” fluorescent sensor for detection of Pb²⁺ based on GQDs and gold nanoparticles (AuNPs). The mechanism of detection is due to the fluorescence recovery from the separation of GQDs and AuNPs induced by adding Pb²⁺. The proposed fluorescence sensor possesses an extremely broad detection range with a low detection limit, which achieves simply and inexpensively quantitative analysis of Pb²⁺.

DNAzyme (catalytic strand) are main members of functional nucleic acids which can either bind to a target molecule or perform catalytic reactions with the ability to recognize metal ion [24]. In 2003 Brown reported a DNAzyme, which could be binding Pb²⁺ and result in catalytic hydrolysis of the oligonucleotide [25]. Then a series of reports have been presented based on the DNAzyme for detection of Pb²⁺. Tang et al. developed an enzyme-free electrochemical sensor for detection of Pb²⁺ base on the particular DNA strands [26]. Zhang et al. reported a photoelectrochemical

* Corresponding author.

E-mail address: luo.d@sustc.edu.cn (D. Luo).

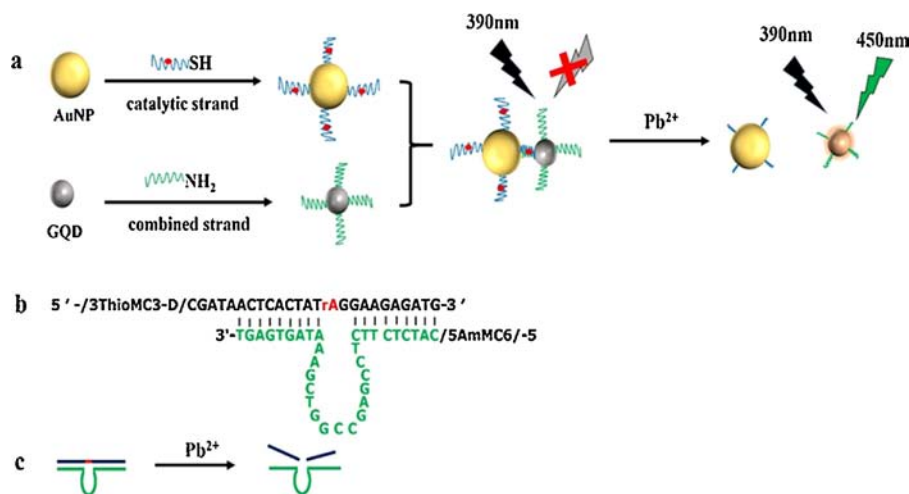


Fig. 1. (a) Schematic illustration of Pb²⁺ detection based on fluorescence resonance energy transfer between GQDs and AuNPs. (b) Structure formula of combined GQDs and AuNPs. (c) Schematic of catalytically cleave of the DNA molecule.

DNAzyme sensor based on ZnO nanoflower for detection of Pb²⁺ by the DNA strands [27]. In this study, catalytic strand and its combined strand were used as the mediums to connect GQDs and AuNPs. Based on strong fluorescence of GQDs, fluorescence quenching between GQDs and AuNPs and fluorescence recovery with the presence of lead ion are used to achieve quantitative analysis of Pb²⁺. Fig. 1(a) shows the schematic illustration for Pb²⁺ detection based on fluorescence resonance energy transfer (FRET) between GQDs and AuNPs [28]. Here, the GQDs were immobilized with amine modified combined strand by 1-Ethyl-3-(3-dimethylaminopropyl) carbodiimide (EDC). Then the AuNPs were modified with catalytic strand by sulfhydryl groups. After mixing each other of the modified particles, a complementary base-pairing reaction took place, leading to the connection of GQDs and AuNPs by catalytic strand (DNAzyme) and combined strand, which was single oligopeptide and modified on GQDs and AuNPs, respectively, (the structural formula is as shown in Fig. 1(b)). Substantial fluorescence quenching will be triggered in the system at the excitation wavelength of 390 nm due to the FRET from GQDs to AuNPs. In appearance of Pb²⁺, the GQDs and AuNPs started to disassemble by catalytically cleaving of DNA molecule due to catalytic activity of catalytic strand [29,30]. The DNA molecule will be catalytically cleaved at the “rA” site, releasing a AuNPs-linked oligonucleotide fragment, a related long oligonucleotide fragment labeled with AuNPs, and a DNAzyme strand with GQDs, as shown in Fig. 1(c). The fluorescence will recovery at wavelength of 450 nm.

2. Materials and methods

In our experiment, Gold (III) chloride trihydrate (HAuCl₄·3H₂O), sodium citrate solution, phosphate buffer solution, EDC, MnCl₂, FeCl₃, KCl, HgCl₂, CuCl₂, MgCl₂, CaCl₂, ZnCl₂, CdCl₂, AgNO₃, and Pb(NO₃)₂ were all purchased from Sigma-Aldrich (St. Louis, MO, USA). Graphene quantum dot (GQD) solution was purchased from Nanjing XFNANO Materials Tech Co., Ltd. (Nanjing, China). The catalytic strand (5′-/3ThioMC3-D/CGATAACTCACTATrAGGAAGAGATG-3′) and combined strand (5′-/5AmMC6/CATCTCTTCTCCGAGCCGGTTCGA-AATAGTGAGT-3′) were purchased from Shenggong Bioengineering Ltd. Company (Shanghai, China). PBS buffer was used for this reaction. The role of this mixture was indicating the preparation process of PBS buffer, which was mixed by 0.1 M NaCl, 5 mM NaHPO₄ and 5 mM Na₂HPO₄. The pH of the buffer was 7.4 and the catalytic strand and AuNPs were added in the PBS buffer in centrifuge tube. All

aqueous solutions were prepared using double-deionized water obtained from a Millipore Ultra-Pure Reagent Water System (Millipore, Continental Water Systems, El Paso, TX, USA). The morphology and size of GQDs and AuNPs were characterized using a Tecnai F30 transmission electron microscopy (TEM). A UV–visible spectrophotometer (Metash, UV-5200PC) was used to measure the absorption spectrum of AuNPs. A fluoroSENS-9003 analytical spectrophotometer was used to measure the emission spectrum of GQDs.

To prepare AuNPs conjugation with combined strand, 1 ml of 24 mM HAuCl₄ was firstly mixed with 98 ml of H₂O and then heated to 110 °C for 5 min, then 10 ml of 14.55 mM trisodium citrate solution was rapidly injected into the solution. The boiling solution was stirred rapidly and refluxed for 20 min. After the color of the solution gradually changed from colourless to wine red, the solution was kept stirring at room temperature for 30 min and then filtered by a 0.22 μm filter. The average size of prepared AuNPs was around 18 nm. 500 μl of AuNP solution prepared was diluted 10 times by adding water and then mixed with the thiol-modified catalytic strand (5′-/3ThioMC3-D/CGATAACTCACTATrAGGAAGAGATG-3′, 100 μM). Next, PBS buffer was slowly added in and left for 16-h standing. The product was centrifuged at 10,000 rpm for 10 min to remove the supernatant unreacted reagents, and the remaining red precipitate was collected at the bottom. The process of GQDs-ssDNA conjugation was following. Firstly, the GQD (1 mg/mL) functionalized with carboxylic acid group was sonicated for 10 min and added by 27 mM EDC. The solution was shaking for 2 min and then sonicated for 30 s. After that, the amine-modified combined strand (5′-/5AmMC6/CATCTCTTCTCCGAGCCGGTTCGA-AATAGTGAGT-3′, 100 μM) was added into the solution at, the solution was incubated for 1 h at room temperature.

3. Results and discussion

The AuNPs were synthesized by the citrate reduction method and modified with oligonucleotides strand. A TEM experiment was performed to characterize the morphology and sizes of AuNPs. The average diameter of the monodispersed AuNPs and GQDs was about 18 nm (Fig. 2a) and 5 nm (Fig. 2b), respectively. It can be seen that both AuNPs and GQDs were well dispersed and separated. When the AuNPs and GQDs were conjugated, the distance between GQDs and AuNPs was only several nanometers, as shown in Fig. 2c.

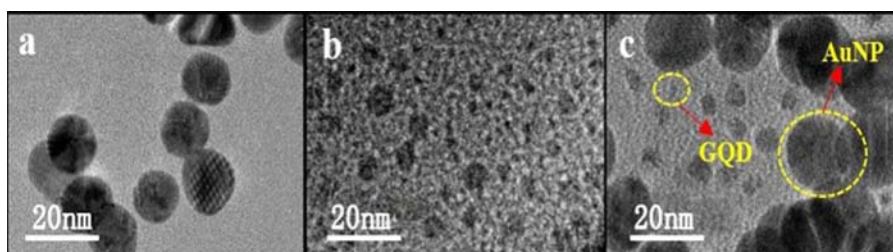


Fig. 2. TEM images of (a) synthesized AuNPs with average size of 18 nm; (b) GQDs with average size of 5 nm; (c) AuNPs conjugated with GQDs. Scale bar: 20 nm.

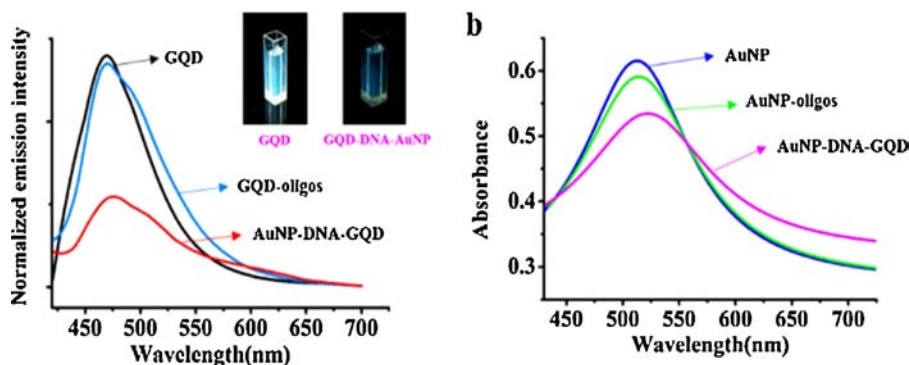


Fig. 3. (a) Emission spectra of GQDs before and after conjugating with oligos (catalytic strand) and AuNPs; (b) absorption spectra of AuNPs before and after conjugating with oligos (combined strand) and GQDs.

The GQDs dispersed in water were colourless. Fig. 3(a) plots the normalized fluorescence spectra of GQD, GQD-catalytic strand, and AuNP-DNA-GQD involved in the detection route. When illuminated by ultraviolet (UV) light with wavelength of 390 nm, the GQD exhibited strong blue light with central emission band at 470 nm (black curve). The emission curve of GQD-catalytic strand kept mostly unchanged relative to that of GQD, as shown in blue curve. Comparison with GQD, a slightly red-shift of peak wavelength as well as a large reduction of fluorescence intensity were observed in AuNP-DNA-GQD, indicating a successful combination of GQD and AuNP and resulting in significant fluorescence quenching. The images of GQD and AuNP-DNA-GQD were demonstrated in the inset figures, where the difference of fluorescence intensity could be easily identified by naked-eyes. Fig. 3b shows the absorbance spectra of AuNPs, AuNP-combined strand, and AuNP-DNA-GQD, respectively. The absorbance peak of AuNPs (blue curve) and AuNP-combined strand (green curve) were both around 518 nm. When the AuNPs were connected with the GQDs, the obtained absorption spectrum was red-shifted to 523 nm with reduced absorbance. As the absorbance center wavelength of AuNPs is related to shape. The neat sphere shape of AuNPs has an absorbance center wavelength at 518 nm. With the shape change, absorbance center wavelength would shift. The AuNPs should contact with other nanoparticles, which must be the GQDs-oligos in the system, due to the existence of a red shifting of AuNPs absorbance (518 nm–523 nm). It suggested that when the GQDs were absorbed on the surface of AuNPs, the surface plasmon resonance (SPR) of AuNPs would increase that reduced the absorbance.

To evaluate the analytical performance for quantitative analysis of Pb^{2+} , we investigated the effect of Pb^{2+} concentration on fluorescence quenching efficiency and fluorescence recovery. A fixed amount (1 mg/mL) of GQD-combined strand was incubated with different concentrations (50 nM–4 μM) of Pb^{2+} with the volumetric ratio of 200:1 for 1 h treatment to disassemble the GQDs and AuNPs at room temperature. After incubation, the fluorescence intensity was measured. Fig. 4a demonstrates the variation of normalized emission spectrum when different concentrations of Pb^{2+} .

It can be seen that with the increase of concentration of Pb^{2+} , the intensity of fluorescence gradually increases. Before the Pb^{2+} was added into the solution, the wavelength of fluorescence emission was at 468 nm and the intensity was as low as 1500 (shown in Fig. 4a). It was indicated that the GQDs was combined with the AuNPs by the interaction of DNA and the fluorescence resonance energy kept transferring to the AuNPs. However, after the Pb^{2+} was added into the solution, the distance between GQDs and AuNPs increased as Pb^{2+} cut off the catalytic strand, resulting in DNA cleavage and fluorescence recovery of GQDs. We can see that the fluorescence intensity of the system was increased with a positive correlation with the concentration of Pb^{2+} from 50 nM to 4 μM . Moreover, a red shift of emission wavelength about 7 nm from 468 nm to 475 nm was observed as well, shown in Fig. 4a. The reason might be that the remainder DNA from AuNPs left on the GQDs and made a larger plasma resonance of GQDs. The relationship between the fluorescence emission intensity and the logarithm of concentration of Pb^{2+} is presented in Fig. 4b. The relative intensity increment with the expression $(F - F_0)/F_0$ shows a dynamic range for Pb^{2+} , which can be expressed by $y = 1.6391x - 2.2219$. We can see that the Pb^{2+} sensor has a broad dynamic range of 50 nM–4 μM with a detection limit of 16.7 nM. Although the detection limit of proposed method is slightly inferior to that based on organic dye (0.4 nM) [31], semiconductor quantum dots (0.09 nM) [32] and graphene quantum dots/graphene oxide (0.6 nM) [33], its detection range (50 nM–4 μM) is 10–400 times broader than those based on organic dye (2–50 nM), semiconductor quantum dots (0.1–10 nM), and graphene quantum dots/graphene oxide (9.9–435.0 nM). The extremely broad detection range of sensor is quite useful to its practice applications.

Selectivity, as another importance performance parameter of sensor in practical application, was evaluated as well. Here, we measured 200 nM Mn^{2+} , Fe^{3+} , K^+ , Hg^{2+} , Cu^{2+} , Mg^{2+} , Ca^{2+} , Zn^{2+} , Cd^{2+} , Ag^+ and 50 nM Pb^{2+} in the system for fluorescence response, as shown in Fig. 5. It can be seen that a sharp increase in fluorescence was induced by 50 nM addition of Pb^{2+} , while no obvious change had been observed after the addition of 200 nM other metal ions.

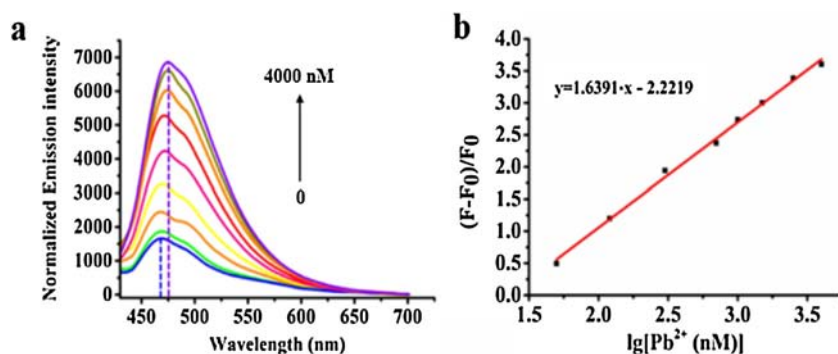


Fig. 4. (a) Fluorescence emission spectra of the sensor after adding various concentrations of Pb^{2+} (from bottom to top: 0, 50, 120, 300, 700, 1000, 1500, 2500 and 4000 nM); (b) Plots of fluorescence signal recovery $(F_0 - F)/F_0$ versus a series of Pb^{2+} concentrations from 50 nM to 4000 nM.

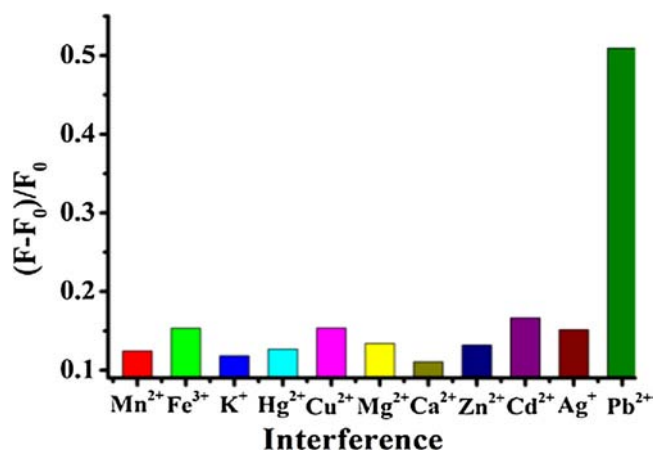


Fig. 5. Selectivity of the sensor in presence of Mn^{2+} , Fe^{3+} , K^+ , Hg^{2+} , Cu^{2+} , Mg^{2+} , Ca^{2+} , Zn^{2+} , Cd^{2+} , Ag^+ (200 nM) and Pb^{2+} (50 nM).

The restoration efficiency of Pb^{2+} was about 3 times to other metal ions. As it is not easy to identify Hg^{2+} and Pb^{2+} separately, this fluorescence sensor is helpful to distinguish these two metal ions. The system has negligible response to Mn^{2+} , Fe^{3+} , K^+ , Hg^{2+} , Ca^{2+} , Zn^{2+} , Cd^{2+} and Ag^+ under the same condition. The result suggests that other ions mentioned above couldn't separate the GQDs and AuNPs. The reason may be that other ions cannot easily cleave the DNA molecule and separate the GQDs and AuNPs, therefore no recovery from quenching process. The result indicates that the sensor possesses a remarkable high selectivity to Pb^{2+} . This is the first time to achieve highly sensitive and selective “turn-on” fluorescent sensor for Pb^{2+} detection based on fluorescence resonance energy transfer between GQDs and AuNPs.

4. Conclusions

In this work, a “turn-on” fluorescence sensor for detection of Pb^{2+} based on graphene quantum dots and gold nanoparticles has been demonstrated. The combination and de-aggregation of GQDs and AuNPs, induced by catalytic strand and lead ion separately, leads to fluorescence quenching and fluorescence recovery. The proposed fluorescence sensor possesses an extremely broad detection range of Pb^{2+} from 50 nM to 4 μM , with a detection limit of 16.7 nM. The sensor also demonstrates highly selectivity of Pb^{2+} from many other metal ions especially Hg^{2+} . This sensing system is highly sensitive and selective for determination of Pb^{2+} . It appears that the GQDs-AuNPs system might provide a new general platform for other heavy metal, antigen, or DNAs in chemical and biological applications by modifying specific sensing molecules.

Acknowledgements

This work is supported by National Natural Science Foundation of China (NSFC) (61405088, and 11574130), Shenzhen Science and Technology Innovation Council (JCYJ20150601155130435, JCYJ20160226192528793, JCYJ20150930160634263, and KQTD2015071710313656).

References

- [1] H.A. Godwin, The biological chemistry of lead, *Curr. Opin. Chem. Biol.* 5 (2001) 223–227.
- [2] A.P.C. Chen, Y.H. Chen, H.P. Liu, Y.C. Li, C.T. Chen, P.H. Liang, Synthesis and application of a fluorescent substrate analogue to study ligand interactions for undecaprenyl pyrophosphate synthase, *J. Am. Chem. Soc.* 124 (2002) 15217–15224.
- [3] H.Y. Lee, D.R. Bae, J.C. Park, H. Song, W.S. Han, J.H. Jung, A selective fluoroionophore based on BODIPY-functionalized magnetic silica nanoparticles: removal of Pb^{2+} from human blood, *Angew. Chem.* 121 (2009) 1265–1269.
- [4] M.P. Ochsenuhn, K.M. Ochsenuhn, Comparison of inductively coupled plasma-atomic emission spectrometry, anodic stripping voltammetry and instrumental neutron-activation analysis for the determination of heavy metals in airborne particulate matter, *J. Anal. Chem.* 369 (2001) 629–632.
- [5] C.R.T. Tarley, F.N. Andrade, F.O. Midori, M. Z. Corazza, L.F. Mendes, M.G. Segatelli, Synthesis and application of imprinted polyvinylimidazole-silica hybrid copolymer for Pb^{2+} determination by flow-injection thermospray flame furnace atomic absorption spectrometry, *Anal. Chim. Acta* 703 (2011) 145–151.
- [6] X. Shi, W. Gu, C. Zhang, L. Zhao, L. Li, W. Peng, Y. Xian, Construction of a graphene/Au-Nanoparticles/Cucurbit [7] uril-based sensor for Pb^{2+} sensing, *Chem. Eur. J.* 22 (2016) 5643–5648.
- [7] S.M. Rosolina, J.Q. Chambers, C.W. Lee, Z.L. Xue, Direct determination of cadmium and lead in pharmaceutical ingredients using anodic stripping voltammetry in aqueous and DMSO/water solutions, *Anal. Chim. Acta* 893 (2015) 25–33.
- [8] Z. Jian, Q.Y. Yun, J.J. Li, J.W. Zhao, Colorimetric detection of lead (II) ions based on accelerating surface etching of gold nanorods to nanospheres: the effect of sodium thiosulfate, *RSC Adv.* 6 (2016) 25611–25619.
- [9] J. Li, Y. Lu, A highly sensitive and selective catalytic DNA biosensor for lead ions, *J. Am. Chem. Soc.* 122 (2000) 10466.
- [10] X. Yang, J. Xu, X. Tang, H. Liu, D. Tian, A novel electrochemical DNAzyme sensor for the amplified detection of Pb^{2+} ions, *Chem. Commun.* 46 (2010) 3107–3109.
- [11] H.N. Kim, W.X. Ren, J.S. Kim, J. Yoon, Fluorescent and colorimetric sensors for detection of lead, cadmium, and mercury ions, *Chem. Soc. Rev.* 41 (2012) 3210–3244.
- [12] B. Trauzettel, D.V. Bulaev, D. Loss, G. Burkard, Spin qubits in graphene quantum dots, *Nat. Phys.* 3 (2007) 192–196.
- [13] L.A. Ponomarenko, F. Schedin, M.I. Katsnelson, R. Yang, E.W. Hill, K.S. Novoselov, A.K. Geim, Chaotic Dirac billiard in graphene quantum dots, *Science* 320 (2008) 356–358.
- [14] K.A. Ritter, J.W. Lyding, The influence of edge structure on the electronic properties of graphene quantum dots and nanoribbons, *Nat. Mater.* 8 (2009) 235–242.
- [15] X. Li, M. Rui, J. Song, Z. Shen, H. Zeng, Carbon and graphene quantum dots for optoelectronic and energy devices: a review, *Adv. Funct. Mater.* 25 (2015) 4929–4947.
- [16] W. Shi, H. Fan, S. Ai, L. Zhu, Preparation of fluorescent graphene quantum dots from humic acid for bioimaging application, *New J. Chem.* 39 (2015) 7054–7059.

- [17] H. Sun, L. Wu, W. Wei, X. Qu, Recent advances in graphene quantum dots for sensing, *Mater. Today* 16 (2013) 433–442.
- [18] G. Konstantatos, M. Badiol, L. Audreau, J. Osmond, M. Bernechea, F.P.G. Arquer, F. Gatti, F.H.L. Koppens, Hybrid graphene-quantum dot phototransistors with ultrahigh gain, *Nat. Nano* 7 (2012) 363–368.
- [19] J. Shen, Y. Zhu, X. Yang, C. Li, Graphene quantum dots: emergent nanolights for bioimaging, sensors, catalysis and photovoltaic devices, *Chem. Commun.* 48 (2012) 3686–3699.
- [20] Z.S. Qian, X.Y. Shan, L.J. Chai, J.J. Ma, J.R. Chen, H. Feng, A universal fluorescence sensing strategy based on biocompatible graphene quantum dots and graphene oxide for the detection of DNA, *Nanoscale* 6 (2014) 5671–5674.
- [21] X. Ran, H. Sun, F. Pu, J. Ren, X. Qu, Ag nanoparticle-decorated graphene quantum dots for label-free, rapid and sensitive detection of Ag⁺ and biothiols, *Chem. Commun.* 49 (2013) 1079–1081.
- [22] I. Al-Ogaidi, H. Gou, Z.P. Aguilar, S. Guo, A.K. Melconian, A.K. Al-kazaz, F. Meng, N. Wu, Detection of the ovarian cancer biomarker CA-125 using chemiluminescence resonance energy transfer to graphene quantum dots, *Chem. Commun.* 50 (2014) 1344–1346.
- [23] S. Zhu, J. Zhang, C. Qiao, S. Tang, Y. Li, W. Yuan, B. Li, L. Tian, F. Liu, R. Hu, H. Gao, H. Wei, H. Zhang, H. Sun, B. Yang, Strongly green-photoluminescent graphene quantum dots for bioimaging applications, *Chem. Commun.* 47 (2011) 6858–6860.
- [24] X. Zhao, R. Kong, X. Zhang, H. Meng, W. Liu, W. Tan, G. Shen, R. Yu, Graphene-DNAzyme based biosensor for amplified fluorescence turn-on detection of Pb²⁺ with a high selectivity, *Anal. Chem.* 83 (2011) 5062–5066.
- [25] A.K. Brown, J. Li, C.M.B. Pavot, Y. Lu, A lead-dependent DNAzyme with a two-step mechanism, *Biochemistry* 42 (2003) 7152–7161.
- [26] S. Tang, W. Lu, F. Gu, P. Tong, Z. Yan, L. Zhang, A novel electrochemical sensor for lead ion based on cascade DNA and quantum dots amplification, *Electrochim. Acta* 134 (2014) 1–7.
- [27] B. Zhang, L. Lu, Q. Hu, F. Huang, Z. Lin, ZnO nanoflower-based photoelectrochemical DNAzyme sensor for the detection of Pb²⁺, *Biosens. Bioelectron.* 56 (2014) 243–249.
- [28] S. Bidault, A. Devilez, P. Ghenuche, B. Stout, N. Bonod, J. Wenger, Competition between Förster resonance energy transfer and donor photodynamics in plasmonic dimer nanoantennas, *ACS Photonics* 3 (2016) 895–903.
- [29] T. Li, E. Wang, S. Dong, Lead (II)-induced allosteric G-quadruplex DNAzyme as a colorimetric and chemiluminescence sensor for highly sensitive and selective Pb²⁺ detection, *Anal. Chem.* 82 (2010) 1515–1520.
- [30] B. Zhang, L. Lu, Q. Hu, F. Huang, Z. Lin, ZnO nanoflower-based photoelectrochemical DNAzyme sensor for the detection of Pb²⁺, *Biosens. Bioelectron.* 56 (2014) 243–249.
- [31] X. Li, G. Wang, X. Ding, Y. Chen, Y. Gou, Y. Lu, A turn-on fluorescent sensor for detection of Pb²⁺ based on graphene oxide and G-quadruplex DNA, *Phys. Chem. Chem. Phys.* 15 (2013) 12800–12804.
- [32] M. Li, X. Zhou, S. Guo, N. Wu, Detection of lead (II) with a turn-on fluorescent biosensor based on energy transfer from CdSe/ZnS quantum dots to graphene oxide, *Biosens. Bioelectron.* 43 (2013) 69–74.
- [33] Z.S. Qian, X.Y. Shan, L.J. Chai, J.R. Chen, H.A. Feng, Fluorescent nanosensor based on graphene quantum dots–aptamer probe and graphene oxide platform for detection of lead (II) ion, *Biosens. Bioelectron.* 68 (2015) 225–231.

Biographies

Xiao-Fang Niu is a laboratory assistant in the Department of Electrical and Electronic Engineering, South University of Science and Technology of China. He received his Master's Degree from Yunnan Normal University in 2014. His research interests include optical analysis, bioanalytical applications, biosensors and functional nanomaterials.

Yuan-Bo Zhong is a laboratory assistant in the Department of Electrical and Electronic Engineering, Southern University of Science and Technology. He obtained his Master's degree of bioengineering in Shenyang Agricultural University in 2016. Now his research interest is focusing on biosensor.

Rui Chen is an associate professor at Department of Electrical and Electronic Engineering, Southern University of Science and Technology. He received his doctoral degree from Nanyang Technological University, Singapore in 2011. His current research interest focuses on the investigation of light and matter interaction based on laser spectroscopy.

Fei Wang received the B.S. degree in mechanical engineering from the University of Science and Technology of China, Hefei, China, in 2003, and the Ph.D. degree in microelectronics from Shanghai Institute of Microsystem and Information Technology, Chinese Academy of Science, Shanghai, China, in 2008. He was a Postdoctoral Researcher with the Department of Microtechnology and Nanotechnology, Technical University of Denmark, where he had been promoted to assistant professor since 2010. Since 2013, he has been an associate professor in the department of Electronic and Electrical Engineering, Southern University of Science and Technology. His current research interests include micro optical sensors, energy harvesting, MEMS and NEMS devices, IC and semiconductor testing.

Yan-Jun Liu is currently an associate professor in the Department of Electrical and Electronic Engineering, Southern University of Science and Technology, China. He received his Ph.D. degree in photonics from Nanyang Technological University, Singapore, in 2007. His research interests are in the fields of active plasmonics and metamaterials, liquid crystal photonics, micro/nano-fabrication.

Dan Luo joined Southern University of Science and Technology in 2013, as an assistant professor in Department of Electrical and Electronic Engineering. He obtained his Ph.D. degree in electronic engineering from Nanyang Technological University (NTU), Singapore in 2012. His research interests include the liquid crystal based tunable photonic devices, liquid crystal laser, holographic polymer dispersed liquid crystal, photonic crystal and quasicrystal, and blue phase liquid crystal.